

# Indirect measurements of neutron-induced reaction cross sections at storage rings

M. Sguazzin<sup>1</sup>, B. Jurado<sup>1\*</sup>, J. Pibernat<sup>1</sup>, J. A. Swartz<sup>1</sup>, M. Grieser<sup>2</sup>, J. Glorius<sup>3</sup>, Y. A. Litvinov<sup>3</sup>, R. Reifarthe<sup>4</sup>, K. Blaum<sup>2</sup>, P. Alfaure<sup>1</sup>, P. Ascher<sup>1</sup>, L. Audouin<sup>5</sup>, C. Berthelot<sup>1</sup>, B. Blank<sup>1</sup>, B. Bruckner<sup>4</sup>, S. Dellmann<sup>4</sup>, I. Dillmann<sup>6</sup>, C. Domingo-Pardo<sup>7</sup>, M. Dupuis<sup>8,9</sup>, P. Erbacher<sup>4</sup>, M. Flayol<sup>1</sup>, O. Forstner<sup>3</sup>, D. Freire-Fernández<sup>2,10</sup>, M. Gerbaux<sup>1</sup>, J. Giovinazzo<sup>1</sup>, S. Grévy<sup>1</sup>, C. J. Griffin<sup>6</sup>, A. Gumberidze<sup>3</sup>, S. Heil<sup>4</sup>, A. Heinz<sup>11</sup>, D. Kurtulgil<sup>4</sup>, G. Leckenby<sup>6</sup>, S. Litvinov<sup>3</sup>, B. Lorentz<sup>3</sup>, V. Méot<sup>8,9</sup>, J. Michaud<sup>1</sup>, S. Perard<sup>1</sup>, N. Petridis<sup>3</sup>, U. Popp<sup>3</sup>, D. Ramos<sup>12</sup>, M. Roche<sup>1</sup>, M.S. Sanjari<sup>3</sup>, R.S. Sidhu<sup>13</sup>, U. Spillmann<sup>3</sup>, M. Steck<sup>3</sup>, Th. Stöhlker<sup>3</sup>, B. Thomas<sup>1</sup>, L. Thulliez<sup>14</sup> and M. Versteegen<sup>1</sup>

<sup>1</sup>LP2I Bordeaux, CNRS/IN2P3-Université de Bordeaux, 33170 Gradignan, France

<sup>2</sup>Max-Planck Institut für Kernphysik, 69117 Heidelberg, Germany

<sup>3</sup>GSI Helmholtzzentrum für Schwerionenforschung, 64291 Darmstadt, Germany

<sup>4</sup>Goethe University of Frankfurt, 60438 Frankfurt, Germany

<sup>5</sup>Université Paris-Saclay, CNRS, IJCLab, 91405 Orsay, France

<sup>6</sup>TRIUMF, Vancouver, British Columbia, V6T 2A3, Canada

<sup>7</sup>IFIC, CSIC-Universidad de Valencia, 46980 Valencia, Spain

<sup>8</sup>CEA, DAM, DIF, 91297 Arpajon, France

<sup>9</sup>Université Paris-Saclay, CEA, LMCE, 91680 Bruyères-Le-Châtel, France

<sup>10</sup>Ruprecht-Karls-Universität Heidelberg, 69117 Heidelberg, Germany

<sup>11</sup>Chalmers University of Technology, 41296 Gothenburg, Sweden

<sup>12</sup>GANIL, 14000 Caen, France

<sup>13</sup>School of Physics and Astronomy, University of Edinburgh, UK

<sup>14</sup>CEA-Paris Saclay, 91191 Gif-sur-Yvette, France

**Abstract.** Neutron-induced reaction cross sections of unstable nuclei are essential for understanding the synthesis of heavy elements in stars. However, their measurement is very difficult due to the radioactivity of the targets involved. We propose to circumvent this problem by using for the first time the surrogate reaction method in inverse kinematics at heavy-ion storage rings. In this contribution, we describe the developments we have done to perform surrogate-reaction studies at the storage rings of GSI/FAIR. In particular, we present the first results of the proof of principle experiment, which we conducted recently at the Experimental Storage Ring (ESR).

## 1 Introduction

Most of the elements from iron to uranium are synthesized in stars via neutron-induced reactions during the slow (s) and rapid (r) neutron-capture processes. Many uncertainties and open questions remain regarding the r-process. For instance, it is not yet clear if the r-process abundance distribution in the solar system is the result of one or multiple scenarios. The

\* Corresponding author: [jurado@cenbg.in2p3.fr](mailto:jurado@cenbg.in2p3.fr)

measurement of neutron-induced cross sections of key neutron-rich nuclei is essential to answer this question [1]. In the neutron-star merger scenario, the fission process plays a significant role [1, 2, 3, 4], since fission sets the end of the r-process path and can significantly impact the abundances in the mass region  $120 < A < 210$ .

A neutron-induced reaction at incident energies below a few MeV can be described as a two-step process (Fig. 1). First, the nucleus  $A$  captures the neutron forming a compound nucleus  $(A+1)^*$ . The excited compound nucleus can then decay in different ways, by emitting  $\gamma$  rays, by emitting a neutron and by fission. Each decay mode has a given probability ( $P_\gamma$ ,  $P_n$ ,  $P_f$ ), and the sum of the probabilities of all the open decay channels must add up to 1.

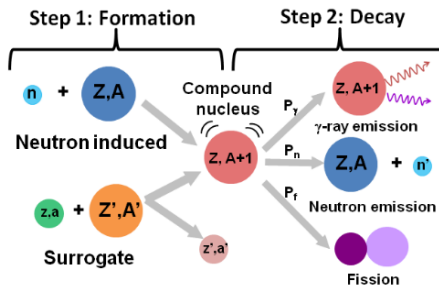


**Fig. 1.** Sequence of a neutron-induced reaction. First a compound nucleus is formed, which then de-excites by the emission of  $\gamma$  rays, a neutron or by fission. The probability  $P$  associated to each decay channel is indicated. In a surrogate reaction, the same compound nucleus as in the neutron-induced reaction is produced by a different reaction.

In traditional neutron-irradiation experiments, the direct measurement of neutron-induced cross sections of short-lived nuclei is very challenging because of the difficulties to produce and handle radioactive targets. Moreover, the associated radioactivity can generate a significant background and can damage the detectors during the measurement. Therefore, when the target nuclei are highly radioactive, experimental data are scarce and most of the neutron-induced reaction cross sections rely on theoretical model predictions. However, these predictions often have very large uncertainties due to difficulties in describing the compound-nucleus de-excitation process (step 2 in Fig. 1). Indeed, the de-excitation process is ruled by fundamental properties (level densities, fission barriers, transmission coefficients, etc.) for which the existing nuclear models give very different predictions. This leads to discrepancies between the calculated cross sections as large as two orders of magnitude or more when no experimental data are available [5].

It is possible to overcome the radioactive-target difficulties by performing the experiments in inverse kinematics with radioactive ion beams. However, this is not yet possible for neutron-induced reactions since free neutron targets are not available. An elegant alternative is to use the surrogate-reaction method in inverse kinematics. The surrogate reaction produces the compound nucleus of interest by a two-body reaction, different than the neutron-induced reaction (see Fig. 1) and the decay probabilities for  $\gamma$  emission, neutron emission and fission are measured as a function of the excitation energy of the compound nucleus. The measured probabilities are used to constrain the fundamental properties mentioned above and enable for much more accurate predictions of the desired neutron-induced cross sections [6, 7, 8].

Using the surrogate-reaction method in inverse kinematics enables for the formation of very short-lived nuclei and for the detection of the heavy, beam-like residues produced after the emission of  $\gamma$  rays and neutrons. However, the decay probabilities change very rapidly with

excitation energy at the neutron separation energy and at the fission threshold. The excitation-energy resolution required to scan this rapid evolution is a few 100 keV, which is quite difficult to achieve for heavy nuclei in inverse kinematics, due to different target issues. Namely, the required large target density and thickness lead to significant energy loss and straggling effects that translate into a large uncertainty for the energy of the projectile and for the emission angle and the energy of the target-like residue. In addition, the presence of target windows and impurities induces background.

In this work, we address the discussed target issues by investigating for the first time surrogate reactions at the ESR storage ring of GSI/FAIR [9]. A key capability of storage rings is beam cooling, which allows for a significant reduction of the size and energy spread of the stored beam. If a gas target is present in the ring, the electron cooler can compensate the energy loss as well as the energy and angular straggling of the beam in the gas target. The ions pass through the target always with the same energy and the same outstanding beam quality. Hence, energy loss and straggling effects in the target are negligible, quite in contrast to single-pass experiments. Moreover, the frequent passing of the target zone (about 1 million times per second at 10 AMeV) allows gas targets with ultra-low density ( $10^{13}$  atoms/cm $^2$ ) to be used and no windows are necessary. This is a great improvement for surrogate reactions since the beam will only interact with the desired material and in a well-defined interaction zone, while the luminosity remains at a high level. Storage rings can be used to reduce the energy of the stored beam from a few 100 AMeV, the typical energy required to produce bare ions, to a few AMeV. This enables another unique feature: the production of 10 AMeV cooled beams of fully-stripped radioactive heavy ions. However, heavy-ion storage rings are operated in ultra-high vacuum (UHV) conditions ( $10^{-10}$  to  $10^{-11}$  mbar), which poses severe constraints to in-ring detection systems. UHV-compatible silicon detectors have only started to be used since a few years for pioneering nuclear-reaction studies at the ESR, see e.g. [10].

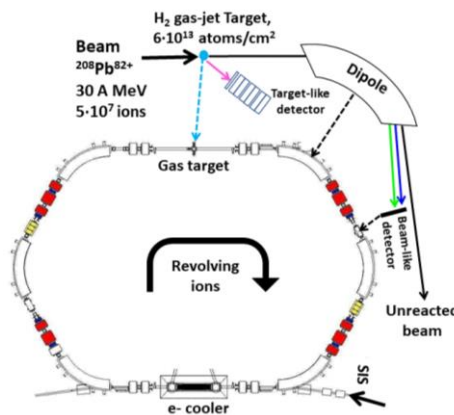


**Fig. 2.** The lower part shows the ESR and the upper part the setup used in our experiment. The trajectory of the scattered protons is shown in pink. The trajectories of the beam-like residues produced after  $\gamma$ -ray ( $^{208}\text{Pb}^{82+}$ ) and neutron emission ( $^{207}\text{Pb}^{82+}$ ) are shown in blue and green, respectively.

## 2 First proof of principle experiment

End of June 2022, we conducted our first proof-of-principle experiment at the ESR storage ring to investigate the  $^{208}\text{Pb}(\text{p},\text{p}')^{208}\text{Pb}^*$  reaction as a surrogate for the  $\text{n}+^{207}\text{Pb}$  reaction. In this experiment, a  $^{208}\text{Pb}^{82+}$  beam at 30.77 AMeV interacted with a gas-jet target of hydrogen. We had on average  $5 \cdot 10^7$   $^{208}\text{Pb}^{82+}$  ions cooled and decelerated per injection and the target thickness was  $6 \cdot 10^{13}$  atoms/cm $^2$ . The  $^{208}\text{Pb}$  projectiles were excited by inelastic scattering

reactions with the target. We measured the inelastically scattered protons with a Si telescope and the beam residues produced after the de-excitation of  $^{208}\text{Pb}^*$  via  $\gamma$ -ray and neutron emission with a position-sensitive Si strip detector placed behind the ring dipole magnet downstream from the target, see Fig. 2. This dipole acted as a recoil spectrometer separating the unreacted beam, the  $^{208}\text{Pb}^{82+}$  residues produced after  $\gamma$ -ray emission and the  $^{207}\text{Pb}^{82+}$  residues produced after neutron emission.

One of the main objectives of this experiment was to evaluate the excitation energy resolution  $\Delta E^*$ . The left part of Fig. 3 shows the energy loss in the telescope versus the residual energy for protons detected at  $64.5^\circ$ . The ground state of  $^{208}\text{Pb}$  is well separated and can be used to evaluate the excitation energy resolution. This is shown on the right part of Fig. 3, where the excitation energy spectrum of  $^{208}\text{Pb}$  for elastically scattered protons is represented. The standard deviation of the ground-state peak is  $\Delta E^* \approx 600$  keV. This resolution agrees with our expectations and is dominated by the angular uncertainty of the scattered protons caused by the large target radius of 2.5 mm. This first experiment has allowed us to validate our simulations, which predict  $\Delta E^* \approx 300$  keV and 200 keV for smaller target radii of 1 or 0.5 mm, respectively. A target with a smaller radius will be available for our next experiments.

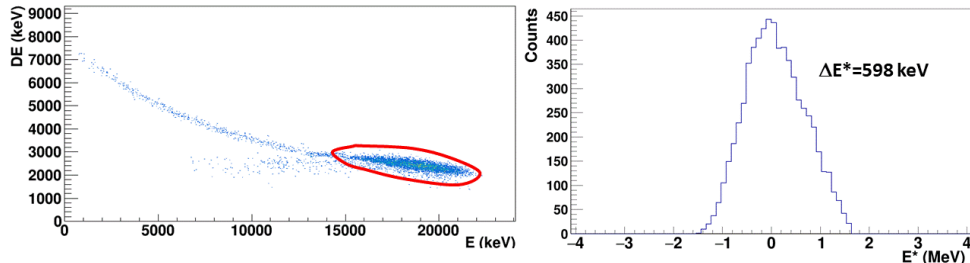


**Fig. 3.** (Left) Preliminary results of the energy loss versus residual energy for scattered protons detected at  $64.5^\circ$ . The red contour selects the elastically scattered protons. (Right) Preliminary results of the excitation energy of  $^{208}\text{Pb}$  for the selected protons. The standard deviation of the peak is indicated.

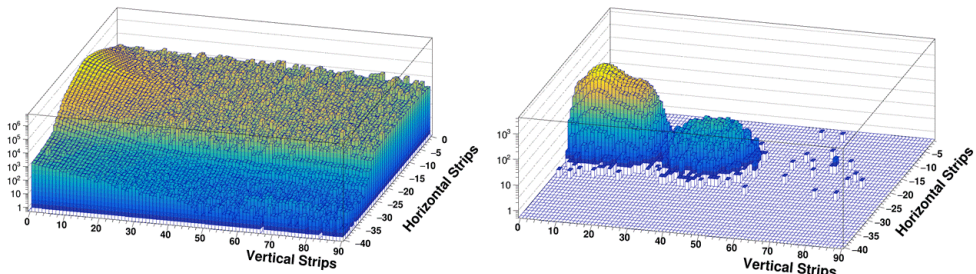


**Fig. 4.** Position of beam residues measured without (left) and with (right) selection of scattered protons detected in the telescope. In the right figure,  $^{208}\text{Pb}^{82+}$  nuclei that de-excite by  $\gamma$  emission are in the left bump, while  $^{207}\text{Pb}^{82+}$  nuclei produced after neutron emission are located in the right bump.

The other main objective of our first experiment was to evaluate the transmission and the separation of the heavy, beam-like residues. Fig. 4 shows the position spectra of heavy residues detected without (left) and with (right) the coincidence with the protons detected in the telescope. Due to the very intense background created by the elastic scattering of the beam, visible in the left part of Fig. 4, the heavy residues of the projectile produced after its de-excitation can only be seen in the coincidence spectrum on the right. The  $^{208}\text{Pb}^{82+}$  nuclei that de-excite by  $\gamma$  emission are in the left bump, while  $^{207}\text{Pb}^{82+}$  nuclei produced after neutron emission are in the right bump. The two bumps are very clearly separated. As expected, the beam residues are detected with very high efficiencies. We detect 100% of the residues

produced after neutron emission and our preliminary analysis shows that we detect between 70 to 96% of the residues produced after  $\gamma$ -ray emission. These efficiencies are much larger than what can be obtained in standard surrogate-reaction experiments in direct kinematics. By counting events in each of the peaks at different  $E^*$  intervals, we will be able to extract for the first time simultaneously the  $\gamma$ - and the neutron-emission probabilities of  $^{208}\text{Pb}$  without the need of measuring  $\gamma$  rays or neutrons. To our knowledge the neutron emission probability as a function of  $E^*$  has never been measured before for any nucleus.

### 3 Conclusion and perspectives

The surrogate-reaction method is a powerful tool to infer indirectly neutron-induced cross sections of short-lived nuclei. Storage rings offer ideal conditions to use the surrogate reaction method in inverse kinematics. We successfully conducted a first proof-of-principle experiment at the ESR storage ring using the  $^{208}\text{Pb}(\text{p},\text{p}')$  surrogate reaction. We were able to evaluate the excitation energy resolution and confirm the full separation and highly efficient detection of the beam-like residues produced after  $\gamma$  and neutron emission. In the next months, we will determine the decay probabilities for  $\gamma$  and neutron emission and use them to infer the neutron-induced radiative-capture and inelastic-scattering cross sections of  $^{207}\text{Pb}$ .

In the near future, we will complete our setup with fission detectors to measure, in addition to the  $\gamma$ -ray and neutron emission probabilities, the fission probabilities of various U isotopes. After validation of the experimental method, we foresee to indirectly infer the neutron-induced reaction cross sections of many short-lived nuclides. First, we will use primary beams of e.g.  $^{238}\text{U}$  and  $^{208}\text{Pb}$  and nearby secondary beams produced by fragmentation. In the longer term, we aim to explore the region of neutron-deficient actinides and pre-actinides towards the  $N=126$  shell closure. It will be the first time that fission probabilities are measured near a shell closure. These studies will help to provide much better theoretical predictions for the fission barriers and cross sections of neutron-rich nuclei towards the shell closure at  $N=184$ , which are essential for the r-process [2, 3] and not yet accessible to experiments.

### Acknowledgements

This work is supported by the European Research Council (ERC) under the European Union's Horizon 2020 research and innovation programme (ERC-Advanced grant NECTAR, grant agreement No 884715). We thank the 80PRIME program from the CNRS for funding the PhD thesis of MS and the GSI/IN2P3 agreement 19-80. AH is grateful for funding from the Knut and Alice Wallenberg Foundation under KAW 2020.0076.

### References

1. T. Kajino et al., *Prog. Part. Nucl. Phys.* **107**, 109 (2019).
2. S. Goriely, *Eur. Phys. J. A* **51**, 22 (2015).
3. N. Vassh et al., *J. Phys. G: Nucl. Part. Phys.* **46**, 065202 (2019).
4. Y. L. Zhu et al., *Astrophys. J.* **906**, 94 (2021).
5. M. Arnould et al., *Phys. Reports* **450**, 97 (2007).
6. J. E. Escher et al., *Phys. Rev. Lett.* **121**, 052501 (2018).
7. A. Ratkiewicz et al., *Phys Rev Lett.* **122**, 052502 (2019).
8. R. Pérez Sánchez et al., *Phys. Rev. Lett.* **125**, 122502 (2020).
9. B. Franzke, *Nucl. Instrum. Methods B* **25**, 18 (1987).

10. J. Glorius et al., Phys Rev Lett **122**, 092701 (2019).